Thermal diffusivity measurements by photothermal and thermographic techniques

F. Cernuschi•, P.G. Bison°, A. Figari•, S. Marinetti° and E. Grinzato°

•*CESI, via Reggio Emilia 39, 20090 Segrate (MI), Italy*
°*CNR-ITC sec. Padova, C.so Stati Uniti 4, 35127 Padova, Italy*

Abstract

In this work, fruit of the collaboration between two laboratories, we present different techniques to measure thermal diffusivity. At first a brief description of every technique both in the experimental layout and in the processing algorithms is given. After that, results obtained on samples cut from the same block of stainless steel AISI 304, are reported. Uncertainties evaluation of any measurement is reported together with a discussion on the pros and cons of the related technique.

1. Introduction

The knowledge of the thermal conductivity and/or the thermal diffusivity is more and more required in many industrial fields; these are the most important parameters when heat transfer processes are involved.
In the power generation industries, materials are selected primarily considering their thermal properties. The last generation of gas turbines hot path components (typically combustion chamber, transition pieces, rotating blades and vanes) are protected against the hot gases (>1300°C) by a ceramic thermal barrier coating (TBC) with a thickness ranging from 300 μm up to 1 or more millimeters. This porous coating can drastically reduce the temperature of the internally cooled metallic base material of 100-300 °C depending on its thickness and on its microstructure. The selection of the best insulating coating allows one to significantly increase the efficiency of the gas turbine because either the cooling flow can be reduced or a higher turbine inlet temperature (TIT) can be achieved [1].
The development of innovative ultra high heat exchangers working at gas temperature higher than 1400 °C is strictly related to the mechanical and thermal properties of innovative ceramic matrix composites (CMC). The first prototype of heat exchangers have been realized by using high thermal conductivity ceramic materials like silicon carbide SiC/SiC or C/CSiC. Usually the value of the thermal diffusivity of the CMC has to be experimentally determined because the fibers within the components are oriented in a complex way. Therefore a proper selection of the material with the best thermal conductivity and a suited design of the heat exchanger piping from the thermo-mechanical point of view can be performed [2-3].
Mechanical, electromagnetic and thermo-physical properties of metallic materials either in form of bulk components or coatings play a key role in the development of resonant cavity for a linear proton accelerator. In particular, the thermal diffusivity at very low temperatures of materials like copper and niobium is often required [4].

CMC SiC/SiC materials are presently under study as a possible solution for manufacturing some fusion reactor components. Also in this case the knowledge of thermal diffusivity of CMC can contribute to help the designers in the selection of the best-suited fiber reinforced composite [5].
In the automotive and aeronautical industries, CMC materials for high performance brakes and heat shields are under development and manufacturers require, as essential information for the optimization of the brake design, the thermal diffusivity of the C/C fibers reinforced disks that have been already installed in some top car models [6].
In civil engineering, the thermal conductivity of concrete used for dams (mainly for hydroelectric power plants) or for storage tanks for liquid gases has been accurately characterized [7].
High temperature thermal conductivity of paints is often required in Lost Foam Casting (LFC). In fact in LFC some refractory coatings based on mica and aluminium silicate and mica refractories are used to guarantee simultaneously high gas permeability and low thermal conductivity necessary to obtain a good quality aluminium castings employing the expanded polystyrene as model for the casting [8].
Although the parameter involved in stationary heat conduction processes is the thermal conductivity *k*, it is a consolidated practice to experimentally evaluate the thermal diffusivity α by transient methods and to calculate indirectly the conductivity by the equation $k = \alpha \rho C$, where the specific heat C and the volumic mass ρ should be known.
This approach has been often suggested because the thermal diffusivity measurement is usually less time consuming and more productive, if compared with the stationary techniques used for thermal conductivity measurements; these techniques for thermal conductivity evaluation require the heat flux measurement that is long, difficult to control and not much accurate. Moreover, the transient techniques, developed for thermal diffusivity measurement, require smaller sample dimensions and can operate in a wide temperature range. In fact, thermal diffusivity methods have been successfully applied from very low temperatures up to 3000°C.
Another advantage of measuring the thermal diffusivity instead of the thermal conductivity is related to the possibility of satisfying the condition of constant temperature during the measurement, being typical temperature variations during the measurement smaller than 1-2°C [9-10].
The methods for the thermal diffusivity measurement proposed over the last four decades, belong mainly to photothermal and photoacoustic [11,12] techniques. Nowadays, the laser flash [13] results the most worldwide applied photothermal technique. In particular in many countries, Laser Flash is currently considered a standard for thermal diffusivity measurement of solid materials [14-16].
This method consists in heating the front face of a sample (typically a small disk shaped specimen) by a short laser pulse and in detecting the temperature evolution on its rear surface. The main advantages of this method are the simplicity and rapidity of the measurement, the possibility to measure the thermal diffusivity on a wide range of materials and within a wide temperature range. On the other hand, though the thermal diffusivity of one layer belonging to a multilayer specimen can be still determined (if the thermophysical properties and the thickness of the other layers are well known), the experimental uncertainty related to the experimental data reduction tends to grow up. One other possible disadvantage of this technique depends on the requirement to extract or to manufacture a sample with well-specified dimensions and thickness. Furthermore,

in some cases it is required, or at least suggested, to carry out thermal diffusivity measurements directly on components.
Other photothermal and photoacoustic techniques working in the one side configuration (i.e. the temperature monitoring is carried out on the heated surface) could in principle overcome these limitations. In particular, Thermal Waves Interferometry (TWI) has been widely applied to measure the thermal diffusivity of single and two layers samples without any specific requirement on the sample dimensions and needing only few information about the thermophysical properties of the substrate material [17-22]. TWI in one-dimensional approximation is based on the periodical uniform heating of the front surface (typically by a modulated laser beam). The two layer structure of coated samples (for single layer samples, air can be fixed as substrate) produces a change of ac-component of the temperature with respect to an uncoated thermally thick sample that can be detected by an IR detector.
TWI in the three-dimensional approximation and the Optical Beam Deflection (e.g. the so called “mirage”) techniques have been successfully applied to measure the in-plane thermal diffusivity of bulk materials [23-30]. In both cases, the laser beam is focused on the sample surface and by scanning the thermal wave field along positions lying outside the beam on a straight line crossing the center of the heating spot, the thermal diffusivity can be determined. The two techniques differ in the detection system. In particular in TWI, the detection of the thermal wave field is obtained by an IR detector while in the OBD, the detection is usually performed by monitoring (by a position sensor) the periodical deflection of a probe laser beam.
The OBD seems to be one of the most accurate and reliable technique but its principal drawback is related to the sample surface preparation. As a matter of fact a very flat and regular surface is required.
In the last years, thanks to the significant progress in infrared technology as well as in electronics, some thermographic techniques for the in-situ thermal diffusivity evaluation have been developed starting from the experience matured in the framework of photothermal techniques, whose applications are generally confined to the laboratories.
In the literature, thermographic methods typically for measuring in-plane thermal diffusivity in bulk materials are reported. All these methods exploit the in-plane heat diffusion which takes place after that a non uniform heating has been imposed. Masking a portion of the sample surface during the heating [31-33] or using a spot- or line-wise heating source [34-38] are the two main ways to generate a planar heat diffusion.
Thermographic TWI in-plane experiment has been used to image the thermal waves and to measure the in-plane thermal diffusivity [39].
In order to verify from the end-user point of view the advantages, the limitations as well as the uncertainty sources, the reliability and the accuracy of some of these photothermal and thermographic techniques, a round robin test between the Istituto per la Tecnologia delle Costruzioni (ITC) of the Italian National Research Council and CESI (Centro Elettrotecnico Sperimentale Italiano) has been launched. In particular, the experimental activity has been limited to some samples extracted by the same plate of the stainless steel AISI304. The final aim of this work is to show that some of these techniques could be considered as a standard for the thermal diffusivity measurement.

2. The techniques

2.1 The laser flash method

2.1.1 Theoretical background

The Laser Flash method is based on the analytical solution of the heat conduction problem within a infinite plate of thickness L, initially at a uniform temperature and uniformly heated on one surface by a Dirac (i.e. instantaneous) energy pulse. The temperature on the rear face of the plate as a function of time is:

$$T(L,t) = \frac{Q}{\rho CL}\left[1 + 2\sum_{n=1}^{\infty}(-1)^n \exp\left(-\frac{n^2\pi^2\alpha t}{L^2}\right)\right] \quad (1)$$

where Q is the heating energy density. Indicating with $T_\infty = \frac{Q}{\rho CL}$ the equilibrium temperature and with $t_c = \frac{L^2}{\alpha}$ eq.(1) can be written as :

$$V(t) = \frac{T(L,t)}{T_\infty} = 1 + 2\sum_{n=1}^{\infty}(-1)^n \, exp(-n^2\pi^2 t / t_c) \quad (2)$$

Figure 1 represents graphically eq. (2).

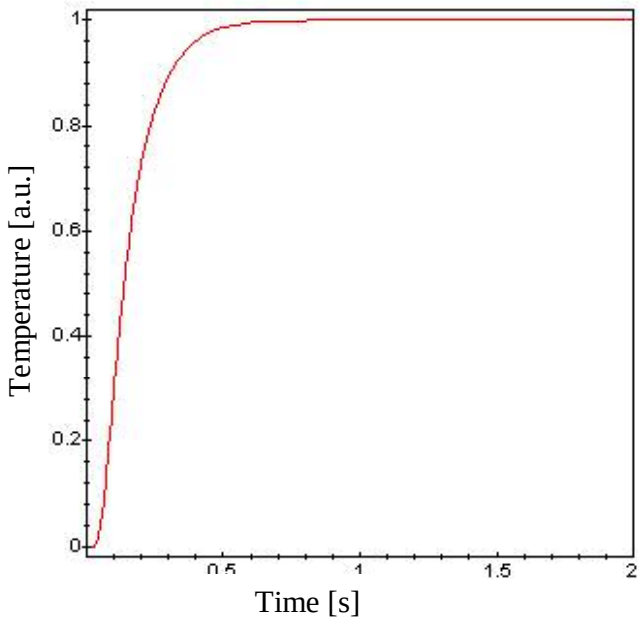

Fig. 1 V(t) vs. the normalised time t/tc.

For evaluating the thermal diffusivity, the solution proposed originally by Parker et al. [12] consisted in using the following relation:

$$\alpha = 0.1388 \frac{L^2}{t_{1/2}} \tag{3}$$

where $t_{1/2}$ is the time corresponding to the half maximum increase of V(t). Relationships analogous to eq.(3) can similarly be obtained for times $t_{x\%}$ corresponding to different percentages of the maximum temperature increase [8]. An other alternative method consists in fitting the whole experimental data by eq.(2). The comparison between all these different methods of data reduction carried out on a wide set of experimental results has shown a very good agreement when the experimental conditions fit well the theoretical assumptions [40].

2.1.2 Experimental set-up and the results

The experimental system shown in figure 2 uses a pulsed 1.06 μm wavelength Nd:YAG laser (Laser Metrics Winterpark FL-USA) as heating source. The pulse energy can be tuned in the range 8-50 J. The beam shape is circular with a uniform intensity. Sample can be allocated within a tantalum furnace with molybdenum shield (Theta Instruments. Port Washington, NY-USA) where it is possible to reach 1500°C. The sample and the furnace are both inside a vacuum chamber and an infrared detector can detect the temperature of the rear face of the sample through an infrared window. The signal is then amplified, acquired and processed by a PC.

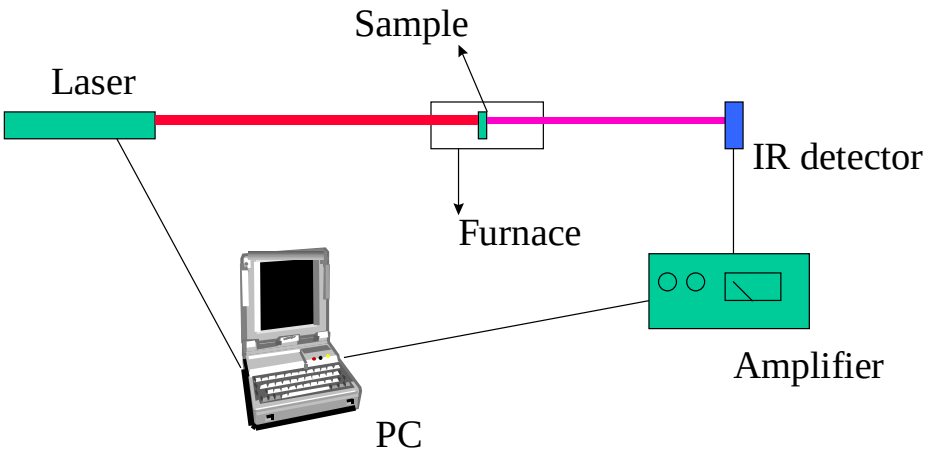

Fig. 2. Sketch of the experimental set-up of the Laser Flash system.

The experimental activity has been carried out on a 10 mm diameter disk shaped sample 1474 μm thick. Measurements have been carried out five times and the associated uncertainty is indicated together with the average result in table 1. Typical experimental profile is shown in figure 3.

2.2 The TWI method

2.2.1 Theoretical background

Thermal wave Interferometry is a well-established technique for measuring the thermal diffusivity of coatings and thin slabs. The propagation of thermal waves with angular frequency ω generated within a two layers solid is affected by the interface between the first and the second layers. In particular thermal waves are partially reflected and transmitted at the separation surface of the two different materials like "conventional" waves. The interference between propagating and reflected waves alters the amplitude and the phase of the ac component of the surface temperature [13]:

$$A = \left(\frac{e^{4h} + 2\Gamma e^{2h}\cos(2h) + \Gamma^2}{e^{4h} - 2\Gamma e^{2h}\cos(2h) + \Gamma^2} \right)^{1/2} \qquad \Delta\phi = \arctan\left(\frac{e^{-2h}(e^{4h} - \Gamma^2)}{2\Gamma \sin(2h)} \right) \tag{4}$$

where $h=L/\mu$ is the normalised thickness of the first layer. $\Gamma = \frac{\varepsilon_1 - \varepsilon_2}{\varepsilon_1 + \varepsilon_2}$ (where $\varepsilon_i = \sqrt{\rho_i C_i k_i}$ is the thermal effusivity) is the thermal wave reflection coefficient at the interface where subscripts 1 and 2 refer to the first and the second layer, respectively. $\mu = \sqrt{\frac{2\alpha_1}{\omega}}$ is the thermal diffusion length and represents the depth where the initial magnitude of the thermal wave reduces by a 1/*e* factor.

Experimentally, the evaluation of the thermal diffusivity α of the first layer can be performed by fitting the experimental data acquired at different modulation frequencies with one of the two expressions of eq.(4). Phase is usually preferred to the amplitude because is less sensitive to optical features of the sample surface as well as to laser power variation during the measurement. As an example, figure 4 shows theoretical curves for phase as a function of the normalised coating thickness *h* for Γ values ranging between -1 and 1 from top to bottom.

2.2.2 Experimental set-up and the results

Figure 5 shows the TWI experimental set-up: the heating source was a 5W Ar ion laser (Spectra Physics 2020). The intensity was modulated using a high stability mechanical chopper (HMS ElektroniK mod. 220-RG). The laser beam was expanded on the sample surface in order to guarantee the one-dimensional approximation. The monitoring of the ac-component of the surface temperature was performed by an $Hg_{1-x}Cd_xTe$ infrared detector (EG&G Judson,). The signal was amplified by a dc-coupled low noise transimpedance preamplifier and than by a lock-in amplifier (EG&G mod. 5501). A time averaging procedure with statistic treatment of the data and subsequent coating thermal diffusivity evaluation was performed under the control of a proprietary PC program.

In this specific case, measurements were carried out on a thin AISI304 slab 660 μm thick modulating the heating source in frequency range 1-20 Hz as also shown in figure 6. The uncertainty associated to the thermal diffusivity value reported in table 1 is

related to the standard deviation of three repeated measurements. Moreover, the statistical uncertainty of the measurement was further reduced by using recipes of ref. 19. In particular, at each frequency thirty statistically independent phase shift values were averaged and the error bars in figure 6 refer to the standard deviation (always smaller than 0.5 deg) computed starting from these data. Since a single frequency scanning measurement yields a sequence of averaged data, in principle by using the error propagation theory it would be possible to estimate the uncertainty in the thermal diffusivity evaluation associated to a single test. However in this work a different approach has been applied as previously explained.

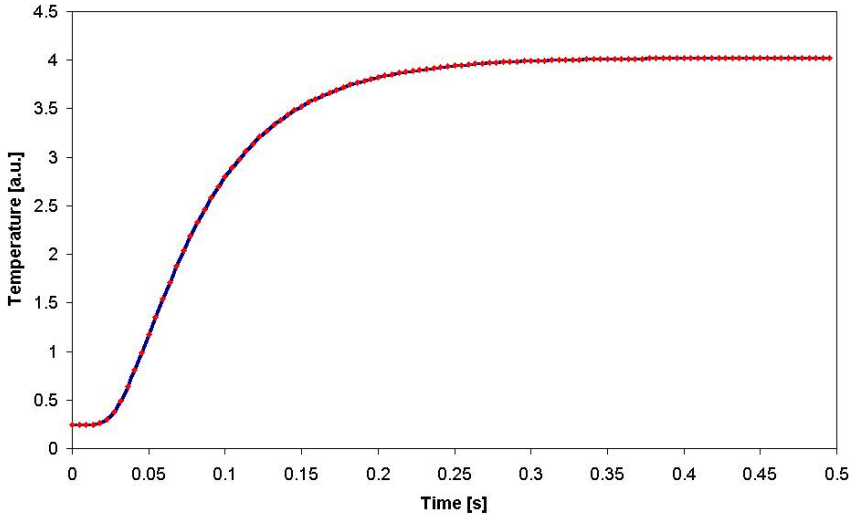

Fig. 3. Temperature increase vs. time in a laser flash experiment for one of the five measurements carried out on the AISI304 stainless steel disk shaped sample. Red dots are experimental points and the blue continuos line is the fitting by using the eq.(2).

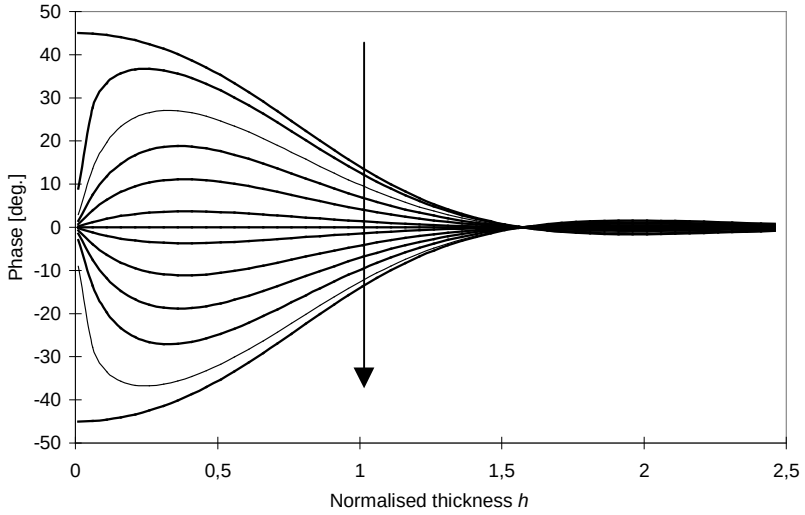

Fig. 4. Phase of the ac component of temperature versus the normalised thickness *h* for different values of the reflection coefficient Γ ranging from -1 to 1 (in the sense of the arrow).

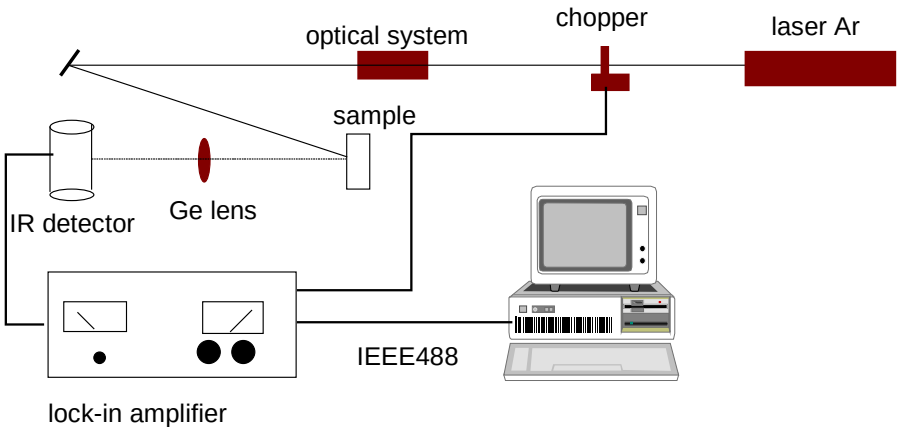

Fig. 5. TWI experimental set-up.

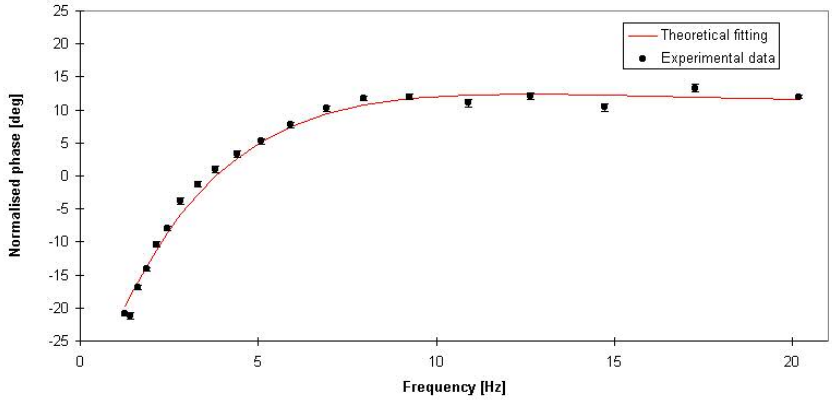

Fig, 6. Normalised phase of the ac component of the surface temperature versus the modulation frequency for the AISI304 sample.

Table 1 Experimental and literature values of thermal diffusivity values for AISI304 stainless steel

Technique	Experimental Value
Literature value (www.matls.com)	$0.040*10^{-4} m^2/s$
Laser Flash	$0.0399\pm0.0006*10^{-4} m^2/s$
TWI	$0.040\pm0.001*10^{-4} m^2/s$
Thermographic method I (two side conf.)	$0.040\pm0.006*10^{-4} m^2/s$
Thermographic method I (one side conf.)	$0.040\pm0.005*10^{-4} m^2/s$
Thermographic method II	$0.0398\pm0.0006*10^{-4} m^2/s$
Thermographic method III	$0.040\pm0.004*10^{-4} m^2/s$

2.3 The Thermographic method I (spatially resolved method)

2.3.1 Theoretical background

The temperature on the front (z=0) and the rear (z=L) surfaces of a semi-infinite slab after an instantaneous spatially Gaussian shaped heating are respectively [37]:

$$T\ (r,0,t) = \frac{2Q}{\varepsilon\sqrt{\pi^3 t}} \sum_{n=-\infty}^{\infty} \exp(-\frac{\left((n-1)L\right)^2}{\alpha t} \frac{1}{\left(R^2+8\alpha t\right)} \exp\left(-\frac{2r^2}{R^2+8\alpha t}\right) \quad (5)$$

$$T\ (r,L,t) = \frac{2Q}{\varepsilon\sqrt{\pi^3 t}} \sum_{n=-\infty}^{\infty} \exp(-\frac{\left((2n-1)L\right)^2}{4\alpha t} \frac{1}{\left(R^2+8\alpha t\right)} \exp\left(-\frac{2r^2}{R^2+8\alpha t}\right) \quad (6)$$

Figure 7 shows the spatial distribution of the temperature as a function of the distance *r* from the spot center for the rear slab surface at different times. Computations have been performed by using the thermal diffusivity and thermal effusivity values of AISI304 stainless steel (ε=8049 $Jm^{-2}s^{-1/2}K^{-1}$ α=0.04*10^{-4} m^2s^{-1}) and fixing the beam radius *R*= 5 mm and slab thickness *L*=1 mm. The term:

$$\frac{1}{2\pi} \frac{1}{\left(R^2+8\alpha t\right)} e^{-\frac{2r^2}{R^2+8\alpha t}} \quad (7)$$

in both eq.(5) and eq.(6) is related to the finite size of the heating beam and it is used for the measurement of the in-plane thermal diffusivity. In particular the proposed technique consists in best fitting (by using a Gaussian function), at some times, the spatial profile of the temperature along a line passing through the center of the heated spot on front or rear sample surface depending to the adopted configuration. In fact the shape of the temperature profile at every fixed time depends only on the Gaussian term in Eq.(7). The angular coefficient of the straight line describing the Gaussian widening as a function of time is eight times the thermal diffusivity of the material:

$$b^2 = R^2 + 8\alpha t \quad (8)$$

Note that neither initial time nor beam radius and sample thickness estimation were required.

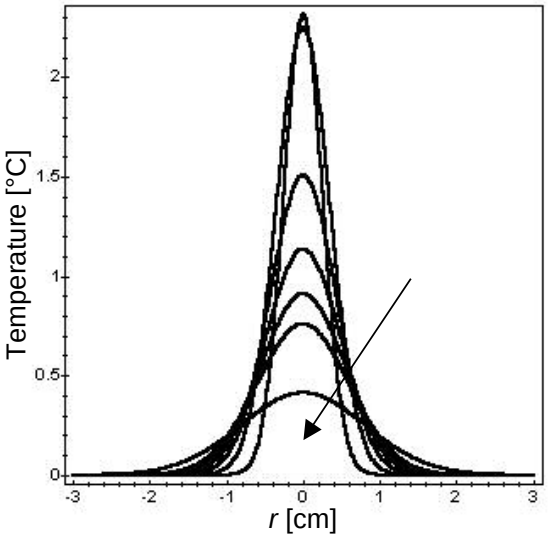

Fig. 7. Eq. (6). *T(r,L,t)* as a function of the distance *r*. Curves refer to time values ranging from 1 to 10 seconds increasing in the direction of the arrow. Computations have been performed by using the energy Q=1 J for a 5.5 mm diameter Gaussian spot.

2.3.2. Experimental set-up and results

The experimental set-up consists in a 1000 W continuous lamp (PSC 1000, ILC Technology Inc. CA) electronically shuttered as heating source and of an infrared Jade Focal Plane Array camera (CEDIP, Crossy-Moligny, F) sensitive in the spectral range 8-10 mm for monitoring the surface temperature distribution of the sample. The sample was a 30x30 cm AISI304 stainless steel plate 1.7 mm thick. The measurements have been performed both in transmission (heating of front surface and temperature monitoring on the rear surface) and in reflection (heating and temperature monitoring of the front surface) configuration. The result and its uncertainty from several tests are reported in table 1. As example, figure 8 and figure 9 show, in the one side configuration, the temperature profile along a diameter 100 ms after the heating pulse and the straight line fitting the experimental data respectively. As far as the geometrical calibration is concerned, after the experiment a razor blade has been placed on the plate surface. This kind of blade is reflecting (thus clearly distinguishable from the black background of the plate) and its edges are parallel and particularly sharp. The measure has been carried out along the longest dimension in order to minimize the errors. Moreover, repeated measurements allow to further reduce the uncertainty in these measurements. In this specific case, the uncertainty related to the geometrical calibration is of ±0.5 pixels on about 110 pixels corresponding to a relative uncertainty lower than 1%.

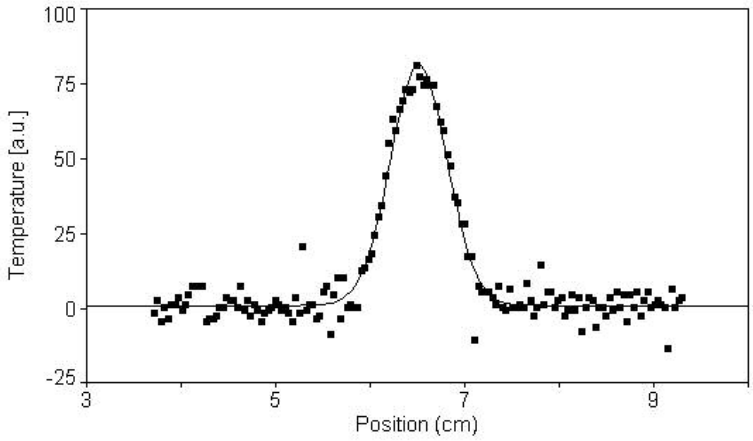

Fig. 8. Temperature vs. position along a line crossing the centre of the Gaussian heating spot 100ms after the heating. The dots are the experimental data while the best fitting Gaussian (with a correlation coefficient r^2=0.958) is represented by the continuos line.

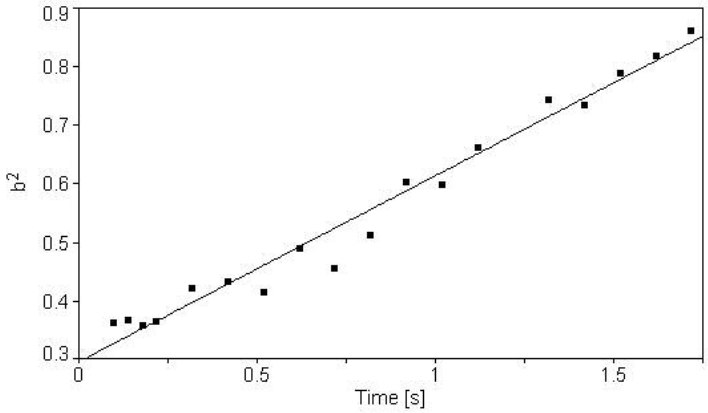

Fig. 9. The best fitting parameter b^2 as a function of the time. Dots and continuos line represent the experimental data and the best fitting (with a correlation coefficient r^2=0.973) straight line respectively.

2.4. The Thermographic method II (lateral thermal waves)

2.4.1. Theoretical background

The thermal model adopted to describe the proposed experimental set-up is the original one due to Ångström [41-43]. It describes the temperature along a semi-infinite bar heated by a periodic source on one end, exchanging heat with the environment and being thermally thin. Therefore temperature varies only down to the bar (1D diffusion) according to the following equation:

$$\Delta T(x,t) = \sum_{n=0}^{N} A_n \exp(-k_{1n}x)\sin(n\omega t - k_{2n}x + \psi_n)$$

$$\Delta T(x,t) = T(x,t) - T_{env}\nu = \frac{\gamma p}{Sc_p\rho} \tag{9}$$

$$k_{1n} = \sqrt{\frac{\nu + \sqrt{\nu^2 + n^2\omega^2}}{2\alpha}}\, k_{2n} = \sqrt{\frac{\nu - \sqrt{\nu^2 + n^2\omega^2}}{2\alpha}}$$

where $T(x,t)$ is temperature function depending on x coordinate along the bar and time t, T_{env} the environment temperature, A_n the amplitude of the n_{th} harmonic component, ω the angular frequency, α is the thermal diffusivity, γ heat exchange coefficient, p and S perimeter and cross-section area of the bar respectively, c_p and ρ specific heat and volumic mass, and ψ_n the initial phase of the n_{th} harmonic component.

The goal of the data reduction procedure consists in determining the spatial phase velocity k_{2n} and the attenuation coefficient of the harmonic component k_{1n}. Hence, the diffusivity α and heat exchange related parameter ν are given by:

$$\alpha = \frac{n\omega}{2}\frac{1}{k_{1n}k_{2n}} \qquad \nu = \frac{n\omega}{2}\frac{k_{1n}^2 - k_{2n}^2}{k_{1n}k_{2n}} \tag{10}$$

2.4.2. Experimental set-up and results

A slab of AISI 304 with dimension 40*250*1.5 mm is used. Height (40 mm) is equal to the side of a thermoelectric device (40*40 mm) that is in contact with the surface on one end of the bar. Driven by a power supply controlled by a PC, it generates the thermal waves. After some cycles the steady regime is reached and the temperature of the surface is grabbed through the IR camera (see figure 10 for the experimental lay-out). The acquisition is repeated at a regular time interval for some periods of the thermal wave. Temperature is finally sampled for each pixel along the propagation path of the thermal wave. As shown in figure 11 the sinusoidal temperature is dumped and phase shifted as the space position increases. The first step of the data reduction procedure consists in time fitting these sine temperature data obtaining amplitude and phase that depend on space. After that, a second fit along the space is done on both amplitude and phase giving finally the dumping factor and the phase velocity of the thermal wave. Measurements were done at different periods of the harmonic heating/cooling flux, and they are condensed in table 1.

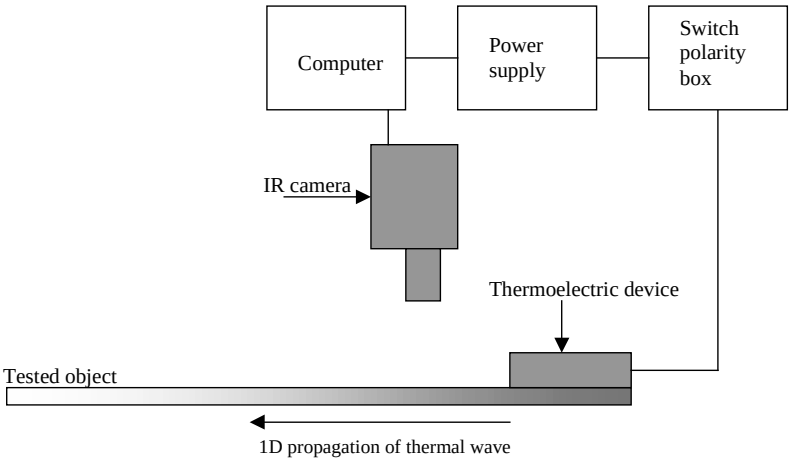

Fig. 10. Experimental set up for diffusivity measurements by thermoelectric generated thermal waves.

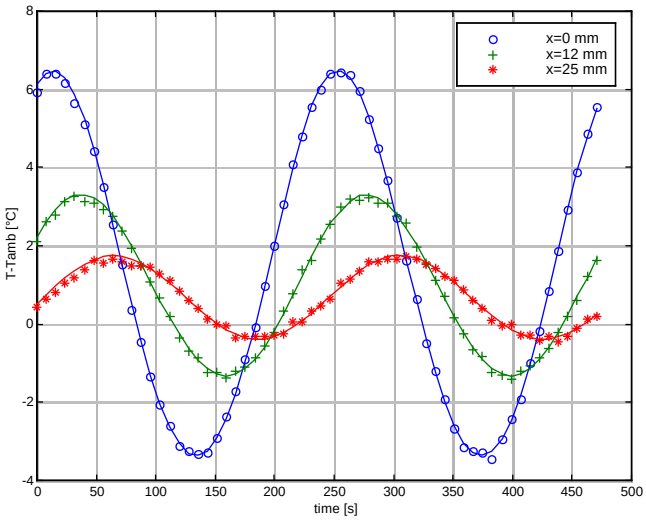

Fig. 11. Temperature vs time at increasing distances from the source/sink thermoelectric device, with fitting function superimposed (continuous line)

2.5. The Thermographic method III (one side flash method)

2.5.1. Theoretical background

It is very interesting to analyze the possibility to measure diffusivity in reflection mode by flash heating. The solution for the heated side of the slab is that given in eq. (1) but for the term $(-1)^n$. For the rear side it gives the alternate signs of the series terms making the solution increasing monotonically. For the front side the lack of such a term makes the solution decreasing monotonically from the maximum temperature value after the flash to the T_∞ value. Unfortunately, the temperature reached during or immediately after the flash is not a reliable value to measure and therefore we cannot extract a noticeable time from the amplitude evolution much like in eq. (2). On the other

hand it is possible to show that multiplying the solution of the front side by the cube root of the time, such a function presents a minimum (that can be measured more easily) at Fo=0.2656 ($Fo=\alpha t/L^2$) giving the following relation for the diffusivity measurement:

$$\alpha = \frac{0.2656\, L^2}{t_{\min}} \tag{11}$$

2.5.2. Experimental set-up and the results

The experimental set-up is shown in figure 12. Two photographic flash lamps, 4800 J nominal energy delivered in about 10 ms, heat one side of the AISI 304 slab, 1.51 mm thick. Temperature is grabbed along a line on the heated surface from an AGEMA 900 LW system for about 2 s with a sampling frequency of 2550 Hz. Figure 13 shows the plot of the function obtained multiplying the experimental temperature by the cube root of time. Results and related error obtained by error propagation of eq. (11) is reported in table 1.

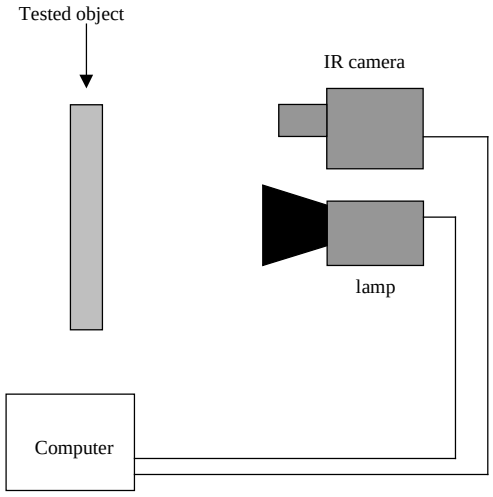

Fig. 12 Experimental set-up for one side diffusivity measurement by flash heating

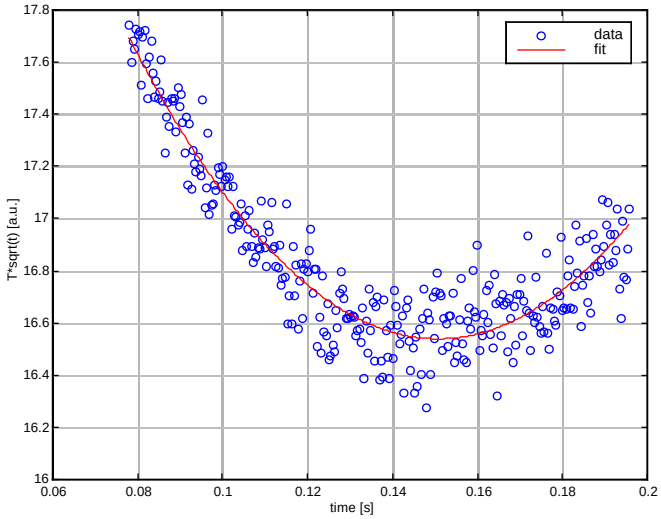

Fig. 13. Data and fitting function to obtain the time of minimum for diffusivity measurement.

3. Conclusion

From the data reported in table 1 it appears that Laser Flash is the reference method for diffusivity measurement as it is currently considered. From the point of view of precision the thermographic method II (lateral thermal waves) gives the possibility to produce thermal waves of large wavelength thank to the peltier driven heat flux. That permits to exploit the capabilities of modern thermographic camera. TWI, the thermographic method III (one side flash) and the thermographic method I (spatially resolved method) are very interesting for their practical feasibility especially in situ, remaining at an acceptable level of precision.

From the point of view of the measurement accuracy for those techniques measuring the through-the-thickness thermal diffusivity, as already highlighted in the literature, good thickness uniformity as well as satisfactory parallelism between the sample faces are essential requirements to fit the theoretical assumptions of the analytical models. Thermographic techniques are mainly affected from the conversion factor between pixel and real length, for this reason a specific care should be given to the definition of procedures for getting this geometrical factor.

Acknowledgements

The authors desire to thank dr. D. Robba and Mr. L. Lorenzoni of CESI for their support to a part of the experimental work.

REFERENCES

[1] V.P. Swaminathan and N.S. Cheruvu, “Gas Turbine Hot-Section Materials and Coatings in Electric Utility Applications”, in *Advanced Materials and Coatings for Combustion Turbines*, Edited by V.P. Swaminathan and N.S. Cheruvu. ASM International, 1994.

[2] European Brite-Euram Project BRPR-CT97-0425 EFCC/UHTHE/B3

[3] European Brite-Euram Project BRPR-CT97-0426 EFCC/UHTHE/B4

[4] G. Penco, D. Barni, P. Michelato, C. Pagani, *Proceeding of Particle Accelerator Conference 2001*, Chicago USA, 2001, p.1231-1240.

[5] A. Donato, A. Ortona, C.A. Nannetti, S. Casadio, "SiC/SiC Fibre Ceramic Composite for Fusion Application: a new Manufacturing Process" *Proc. 19th Symp. on Fusion technology (SOFT)*, Lisbon, (P) Sept. 1996.

[6] TWI Bulletin Nov/Dec. 1996 Reprint 508/6/96

[7] A. Donati, A. Lanciani, P. Morabito, P. Rossi, F. Barberis, R. Berti, A. Capelli, P. G. Sona, *High temp. High Press*. 19, 371, (1987).

[8] T. Mollbog, H. Wang, H.E. Littleton, *AFS Transactions Paper* No: 00-167, pp. 471-478.

[9] R.E. Taylor, K.D. Maglic, *Compendium of Thermophysical Property Measurement Methods Vol: 1: Survey of Measurement Techniques,* Eds. K.D. Maglic et Al. (Plenum Press, New York, 1984), pp. 299-333.

[10] R.E. Taylor, K.D. Maglic, *Compendium of Thermophysical Property Measurement Methods Vol: 2: Recommended Measurement Techniques and Practices,* Eds. K.D. Maglic et Al. (Plenum Press, New York, 1992), pp.281-314.

[11] A. Mandelis, *Progress in Photothermal and Photoacoustic Science and Technology* Vol. 1 (Elsevier, New York, 1991), pp. 207-284.

[12] D.P. Almond, P.M. Patel, *Photothermal Science and Techniques* (Chapman & Hall, London, 1996), pp.199-220.

[13] W.P. Parker, R.J. Jenkins, C. P. Butter G. L. Gutter and G.L. Abbott, *J. Appl. Phys.*, 32, 1679, (1961).

[14] ASTM C714-72 Standard test method for thermal diffusivity of carbon and graphite by a thermal pulse method, ASTM, (1972).

[15] BS7134: Section 4.2: 1990; Method for the determination of thermal diffusivity by the laser flash (or heat pulse) method. British Standards Institution, (1990).

[16] JIS R 1611: Testing methods of thermal diffusivity, specific heat capacity and thermal conductivity for high performance ceramics by laser flash method, Japanese Standards Association (1991).

[17] P.M. Patel and D.P. Almond, *J. Mater. Sci.* 20, 955, (1985).

[18] H.P.R. Frederikse, X.T. Ying and A. Feldman, *Mater. Res. Soc. Symp. Proc.*142, 289, (1989).

[19] L. Fabbri, F. Cernuschi, P. Fenici, S. Ghia and G.M. Piana, in Proceedings of Materials for advanced Power Engineering, Liege, October 1994, edited by D Coutsouradis et al.(Kluwer, Dordrecht, 1994) Part II, pp. 1377-1384.

[20] F. Cernuschi, A. Figari, L. Fabbri, *Journal of Materials Science* **35,** 5891, (2000).

[21] C. Wang, A. Mandelis, *J. Appl. Phys*. **85**, 8366, (1999).

[22] A.C. Bento D.P. Almond S.R. Brown I.G. Turner, *J. Appl. Phys*. **79**, 6848, (1996).

[23] G. Rousset and F. Lepoutre, *Rev. Phys. Appl.* **17**, 201, (1982).

[24] P.K. Kuo, M.J. Lin, C.B. Reyes, L.D. Favro, R.L. Thomas, D.S. Kim, S.Y. Zhang, L.J. Inglehart, D. Fournier, A.C. Boccara and N. Yacoubi, *Can J. Phys.* **64**, 1165, (1986).

[25] P.K. Kuo, E.D. Sendler, L.F. Favro and R.L. Thomas, *Can J. Phys.* **64,** 1168, (1986).

[26] A. Figari, *Meas. Sci. Technol.* **2,** 653, (1991).

[27] A. Figari, *J. Appl. Phys,* **71** (7) 3138, (1992).

[28] A Salazar, A. Sanchez-Lavega and J. Fernandez, *J. Appl. Phys.* **1,** 1216, (1991).

[29] L. Fabbri and P. Fenici, *Rev. Sci. Instrum.* **66** (6), 3593, (1995).

[30] L. Pottier and K. Plamman, *J. Phys*. IV C7, 295, (1994).

[31] J.C. Krapez, in *Proceedings of the 5th Workshop on Advanced Infrared Technology and Applications*, 29-30 September 1999 Venice, Italy, pp.289-296.

[32] I. Philippi, J.C. Batsale, D. Maillet, and A. Degiovanni, *Rev. Sci. Instrum.* **66** (1), 182, (1995).

[33] Zhoung Ouyang, L.D. Favro, and R.L. Thomas in *AIP Conference Proceedings n° 463 Photoacoustic and Photothermal Phenomena*, Rome, August 1998, edited by F. Scudieri and M. Bertolotti (AIP Woodbury, New York,1999) pp. 374-376.

[34] C. S. Welch, D.M. Health, and W. P. Winfree, *J. Appl. Phys.* **61** (3), 895, (1987)

[35] F. Cernuschi, L. Fabbri and M. Lamperti. in *AIP Conference Proceedings n° 463 Photoacoustic and Photothermal Phenomena*, Rome, August 1998, edited by F. Scudieri and M. Bertolotti (AIP Woodbury, New York,1999) pp. 392-394.

[36] D. He, Y. Gu, M. Zheng and D. Zhu, *9th Int. Topical Meeting on Photoacoustic and Photothermal Phenomena*, Nanjing (China), 27-30 June 1996, S.Y. Zhang Ed., Progress in Natural Science, pp. 169-175, (1996).

[37] T. Yamane, S. Katayama, M. Todoki, *Rev. Sci. Instrum.* **67**, (12), 4261, (1996).

[38] F. Cernuschi, A. Russo, L. Lorenzoni, A. Figari, *Rev. Sci. Instrum*. **72**, (19), 3988, (2001).

[39] P.G. Bison, S. Marinetti, A. Mazzoldi, E. Grinzato, C. Bressan. *Infrared Physics & Technology* **43**, 127, (2002).

[40] F. Cernuschi, L. Lorenzoni, CESI Report n° A1/033124 (2001).

[41] A. Ångström, *Philos. Mag*. 25, 130, (1863).

[42] A. Ångström, *Ann. Phys*. (Leipzig) 114, 513, (1861).

[43] H.S. Carslaw and J.C. Jaeger, *Conduction of heat in solids*, (Oxford University Press, London, 1959), pp. 136-139.